



**HAL**  
open science

# Paths Complex Gain Tracking Algorithms for OFDM Receiver in Slowly-Varying Channels

Laurent Ros, Hussein Hijazi, Eric Pierre Simon

► **To cite this version:**

Laurent Ros, Hussein Hijazi, Eric Pierre Simon. Paths Complex Gain Tracking Algorithms for OFDM Receiver in Slowly-Varying Channels. ISCCSP 2008 - 4th International Symposium on Communications, Control and Signal Processing, Mar 2010, Limassol, Cyprus. 6 p. hal-00539149

**HAL Id: hal-00539149**

**<https://hal.science/hal-00539149>**

Submitted on 24 Nov 2010

**HAL** is a multi-disciplinary open access archive for the deposit and dissemination of scientific research documents, whether they are published or not. The documents may come from teaching and research institutions in France or abroad, or from public or private research centers.

L'archive ouverte pluridisciplinaire **HAL**, est destinée au dépôt et à la diffusion de documents scientifiques de niveau recherche, publiés ou non, émanant des établissements d'enseignement et de recherche français ou étrangers, des laboratoires publics ou privés.

# Paths Complex Gain Tracking Algorithms for OFDM Receiver in Slowly-Varying Channels

Laurent ROS, Hussein HIJAZI and Eric Pierre SIMON

**Abstract**—This paper deals with channel estimation for Orthogonal Frequency Division Multiplexing (OFDM) systems over time-varying fading channels. In conventional methods, the least-squares (LS) estimate is obtained over the pilot subcarriers, and next interpolated over the entire frequency grid. Those methods only exploit the frequency-domain correlation of the channel. In this paper, we propose to exploit both the time-domain correlation and the specific features of the wireless radio channel. Assuming the availability of delay related information, we propose to track the variation of the paths complex amplitudes by means of on-line recursive algorithms. We developed two simple sub-optimal algorithms based on second-order loops which exhibit a reduced complexity compared to that of the widely popular Kalman algorithm. The error signal is based on the LS estimate of the path complex gains for the first loop, and on the steepest-descent method of the same LS cost function for the second loop. For each algorithm, we give derivations to correctly tune the loop coefficients. Simulation results over slow Rayleigh fading channel with Jakes' spectrum show that our algorithms outperform the conventional methods. Moreover, the Mean Square Error (MSE) of the first algorithm is closer to the Bayesian Cramer Rao Bound than that of a Kalman filter based on a first-order Autoregressive approximation of the channel.

**Index Terms**—OFDM, Channel estimation, Tracking Loop, Rayleigh channel, Complex gains estimation.

## I. INTRODUCTION

Orthogonal Frequency Division Multiplexing (OFDM) is an effective technique for alleviating frequency-selective fading channels effects in wireless communication systems. In this technique, a wideband frequency-selective channel is converted to a number of parallel narrow-band flat fading subchannels which are free of Intersymbol Interference (ISI) and free (assuming negligible time variations within one OFDM symbol) of Inter-Carrier Interference (ICI). For coherent detection of the information symbols, reliable estimation of the gain of each subchannel in the OFDM system is crucial. Most of the conventional methods work in a symbol-by-symbol scheme by using only the correlation of the channel in the frequency domain (*i.e.* the correlation between subchannels). Generally, they consist in estimating the channel at pilot frequencies and then interpolating the channel frequency response. The channel estimation at the pilot frequencies can be based on Least-Squares (LS) criterion, or for better performance on Linear-Minimum-Mean-Square-Error (LMMSE) criterion [1]. Though the conventional methods can deal with time-varying

channels, the information of the time-domain correlation is not exploited. However, we have shown in [2] through on-line Bayesian Cramer-Rao-Bound (BCRB) analysis, that the channel estimation process of the current symbol can be largely improved by using the previous OFDM symbols. Some works have addressed the time-domain dynamics of the fading process to obtain an updated channel estimate. Chen and Zhang proposed in [3] a structure which uses a Kalman-Filter estimator for each subchannel (exploits the time-domain correlation) and a linear combiner to refine the estimate of each subchannel (exploits the frequency-domain correlation). The complexity of the proposed structure increases with the number of subcarriers. But in practice, only few subcarriers can be used. Another interesting approach to address the problem is to use a parametric channel modeling which can effectively reduce the signal subspace dimension of the channel correlation matrix [4]. Hence, channel estimation can be reduced to the simple estimation of certain physical propagation parameters, such as multi-path delays and multi-path complex gains [4] [5] [6] [7]. Thus, the channel frequency response can be estimated using an  $L$ -path channel model. In [4], the ESPRIT (Estimation of Signal Parameters by Rotational Invariance Techniques) method is employed to acquire the initial multi-path time delays. With this information, a MMSE estimator is derived to estimate the channel frequency response. However, the optimal Wiener estimator remains complex and requires the knowledge of the second-order statistical properties of the channel. In [5], the delay-subspace (assumed invariant over several symbols) is tracked by a subspace-tracking algorithm, and the fast variation of the path amplitudes is tracked separately by a subspace-amplitude tracking algorithm. In [6] [7], we have addressed the problem of path complex gains estimation and ICI reduction for the case of fast-varying Rayleigh channel (normalized Doppler spread  $f_d T \geq 10^{-2}$ ). Based on a polynomial modeling of the (Jakes process) channel gains variation, we use a polynomial estimation over a block of OFDM symbols in [6], and Kalman filtering with Auto-regressive (AR) model for the tracking of the polynomial coefficients in [7]. In fact, a Kalman-based method is quite complex and do not ensure to reach the BCRB in case of mismatch between the AR model and the true channel.

In this paper, we propose simplified multi-path complex gains tracking algorithms based on recursive sub-optimal techniques which closely approach the BCRB in the case of slowly channel variations ( $f_d T \leq 10^{-2}$ ). These algorithms exploit both the time-domain correlation and the specific

L. Ros is with GIPSA-Lab, Image and Signal Department, BP 46, 38402 Saint Martin d'Hères, France (e-mail: laurent.ros@gipsa-lab.grenoble-inp.fr). H. Hijazi and E.-P. Simon are with IEMN lab, TELICE group, 59655 Villeneuve d'Ascq, France (e-mail: hijazihussein@yahoo.com, eric.simon@univ-lille1.fr). This work was supported in part by the ANR project LURGA.

features of the wireless channel. In wireless radio channels, the complex gains show temporal variations while the delays are quasi-constant over a large number of OFDM symbols. Assuming the availability of delay related information as in [6] [7], we propose to track the complex gains variation by means of on-line recursive algorithms. The two proposed algorithms are based on a second-order loop. Thus, complex gains *increments* are also estimated in order to improve the prediction for the next iteration, exploiting the time-domain correlation. The error signal of the first loop is based on the LS estimate of the path complex gains, whereas the error signal of the second-loop is based on the steepest-descent method of the same LS cost function. For each algorithm, we give derivations to correctly tune the loop coefficients. Simulation results compared to the performance of the Kalman filter-based algorithm and to the BCRB validate the proposed algorithms.

The paper is organized as follows: Section II describes the system model. Section III derives the two suboptimal algorithms, whereas Section IV gives the Kalman algorithm. Finally, the different results are discussed in Section V.

*Notations* :  $[\mathbf{x}]_k$  denotes the  $k$ th entry of the vector  $\mathbf{x}$ , and  $[\mathbf{X}]_{k,m}$  the  $[k, m]$ th entry of the matrix  $\mathbf{X}$  (indices begin to 1).  $\mathbf{I}_N$  is a  $N \times N$  identity matrix.  $\text{diag}\{\mathbf{x}\}$  is a diagonal matrix with  $\mathbf{x}$  on its diagonal,  $\text{diag}\{\mathbf{X}\}$  is a vector whose elements are the elements of the diagonal of  $\mathbf{X}$ .  $J_0(\cdot)$  is the zeroth-order Bessel function of the first kind.  $\nabla_{\mathbf{x}}$  represents the first partial derivatives operator *i.e.*,  $\nabla_{\mathbf{x}} = [\frac{\partial}{\partial x_1}, \dots, \frac{\partial}{\partial x_N}]^T$ .

## II. SYSTEM MODEL

### A. OFDM Transmission over multi-path channel

Consider an OFDM system with  $N$  sub-carriers, and a cyclic prefix length  $N_g$ . The duration of an OFDM symbol is  $T = vT_s$ , where  $T_s$  is the sampling time and  $v = N + N_g$ . Let  $\mathbf{x}_{(n)} = [x_{(n)}[-\frac{N}{2}], x_{(n)}[-\frac{N}{2} + 1], \dots, x_{(n)}[\frac{N}{2} - 1]]^T$  be the  $n$ th transmitted OFDM symbol, where  $\{x_{(n)}[b]\}$  are normalized 4-QAM symbols. After transmission over a multi-path channel and FFT demodulation, the  $n$ th received OFDM symbol  $\mathbf{y}_{(n)} = [y_{(n)}[-\frac{N}{2}], y_{(n)}[-\frac{N}{2} + 1], \dots, y_{(n)}[\frac{N}{2} - 1]]^T$  is given by [4] [6]:

$$\mathbf{y}_{(n)} = \mathbf{H}_{(n)} \mathbf{x}_{(n)} + \mathbf{w}_{(n)} \quad (1)$$

where  $\mathbf{w}_{(n)}$  is a  $N \times 1$  zero-mean complex Gaussian noise vector with covariance matrix  $\sigma^2 \mathbf{I}_N$ , and  $\mathbf{H}_{(n)}$  is a  $N \times N$  diagonal matrix with diagonal elements given by:

$$[\mathbf{H}_{(n)}]_{k,k} = \frac{1}{N} \sum_{l=1}^L [\alpha_l^{(n)} \times e^{-j2\pi(\frac{k-1}{N} - \frac{1}{2})\tau_l}] \quad (2)$$

$L$  is the total number of propagation paths,  $\alpha_l$  is the  $l$ th complex gain of variance  $\sigma_{\alpha_l}^2$  (with  $\sum_{l=1}^L \sigma_{\alpha_l}^2 = 1$ ), and  $\tau_l \times T_s$  is the  $l$ th delay ( $\tau_l$  is not necessarily an integer, but  $\tau_L < N_g$ ). The  $L$  individual elements of  $\{\alpha_l^{(n)}\}$  are uncorrelated with respect to each other. Using (2), the observation model in (1) for the  $n$ th OFDM symbol can be re-written as:

$$\mathbf{y}_{(n)} = \text{diag}\{\mathbf{x}_{(n)}\} \mathbf{F} \boldsymbol{\alpha}_{(n)} + \mathbf{w}_{(n)} \quad (3)$$

where  $\boldsymbol{\alpha}_{(n)} = [\alpha_1^{(n)}, \dots, \alpha_L^{(n)}]^T$  is a  $L \times 1$  vector and  $\mathbf{F}$  is the  $N \times L$  Fourier matrix defined by:

$$[\mathbf{F}]_{k,l} = e^{-j2\pi(\frac{k-1}{N} - \frac{1}{2})\tau_l} \quad (4)$$

*Note*: the sub-optimal algorithms proposed in this paper can work without explicit *a priori* random or deterministic model for the path complex gain variations. However, we recall that for the very universal ‘‘Rayleigh model’’, the  $L$  complex gains are wide-sense stationary narrow-band complex Gaussian processes, with the so-called Jakes’ power spectrum [8] with Doppler frequency  $f_d$ . It means that  $\alpha_l^{(n)}$  are zero-means correlated complex Gaussian variables with correlation coefficients given by  $\mathbf{R}_{\alpha_l}^{(p)} = \mathbb{E}[\alpha_l^{(n)} \cdot \alpha_l^{(n-p)H}] = \sigma_{\alpha_l}^2 J_0(2\pi f_d T p)$ .

### B. Pilot Pattern

The  $N_p$  pilot subcarriers are evenly inserted into the  $N$  subcarriers at the positions  $\mathcal{P} = \{p_s \mid p_s = (s-1)L_f + 1, s = 1, \dots, N_p\}$  with  $L_f$  the distance between two adjacent pilots. As we will see with equation (26),  $N_p$  must fulfill the following requirement:  $N_p \geq L$ . The received pilot subcarriers can be written as the sum of two components:

$$\mathbf{y}_{\mathbf{p}(n)} = \text{diag}\{\mathbf{x}_{\mathbf{p}(n)}\} \mathbf{F}_{\mathbf{p}} \boldsymbol{\alpha}_{(n)} + \mathbf{w}_{\mathbf{p}(n)} \quad (5)$$

where  $\mathbf{x}_{\mathbf{p}}$ ,  $\mathbf{y}_{\mathbf{p}}$  and  $\mathbf{w}_{\mathbf{p}}$  are  $N_p \times 1$  vectors, and  $\mathbf{F}_{\mathbf{p}}$  is the  $N_p \times L$  Fourier transform matrix with elements given by:

$$[\mathbf{F}_{\mathbf{p}}]_{k,l} = e^{-j2\pi(\frac{p_k-1}{N} - \frac{1}{2})\tau_l} \quad (6)$$

## III. SUBOPTIMAL TRACKING ALGORITHMS

A tracking algorithm can be defined by an imposed structure, and a specific criteria (or ‘‘error signal’’) to specify some elements of the structure [11]. In the following, we use a second-order recursive structure, and consider two possible error signals, which will lead to 2 possible algorithms.

### A. Structure of the tracking algorithm

*1) Structure*: The purpose is to estimate the channel coefficients  $\boldsymbol{\alpha}$ . The estimate of  $\boldsymbol{\alpha}_{(n)}$ , noted  $\hat{\boldsymbol{\alpha}}_{(n)}$  (or  $\hat{\boldsymbol{\alpha}}_{(n|n)}$ ), is updated at a symbol rate by the computation of a loop error signal  $\mathbf{v}_{\epsilon(n)}$ , which is next filtered by a digital loop filter. Inspired by the Phase-Locked-Loop (PLL) design [12], we use a second-order closed-loop to get the ability to track potential time linear drifts of the parameters to be estimated. The general recursive equations of our loop are :

### Measurement Update Equations

$$\mathbf{v}_{\epsilon(n)} = \text{function of } \{ \mathbf{y}_{\mathbf{p}(n)}; \hat{\boldsymbol{\alpha}}_{(n|n-1)} \} \quad (7)$$

$$\hat{\boldsymbol{\alpha}}_{(n|n)} = \hat{\boldsymbol{\alpha}}_{(n|n-1)} + \mu_1 \cdot \mathbf{v}_{\epsilon(n)} \quad (8)$$

### Time Update equations

$$\mathbf{v}_{\text{Lag}(n)} = \mathbf{v}_{\text{Lag}(n-1)} + \mathbf{v}_{\epsilon(n)} \quad (9)$$

$$\hat{\boldsymbol{\alpha}}_{(n+1|n)} = \hat{\boldsymbol{\alpha}}_{(n|n)} + \mu_2 \cdot \mathbf{v}_{\text{Lag}(n)} \quad (10)$$

where  $\mu_1, \mu_2$  are the (real positive) loop coefficients.

The Measurement Update Equations are responsible for the feedback, *i.e.*, for incorporating a new measurement  $\mathbf{y}_p(n)$  into the *a priori* estimate  $\hat{\boldsymbol{\alpha}}_{(n|n-1)}$  to obtain an improved *a posteriori* estimate  $\hat{\boldsymbol{\alpha}}_{(n|n)}$ . The Time Update Equations are responsible for projecting forward (in time) the current state  $\hat{\boldsymbol{\alpha}}_{(n|n)}$  and error estimates to obtain the *a priori* estimates for the next time step,  $\hat{\boldsymbol{\alpha}}_{(n+1|n)}$ . As in a Kalman filter, the Time Update Equations can also be thought of a predictor equations, while the Measurement Update Equations can be thought of a corrector equations. Note that at each iteration, we get in fact in  $\mu_2 \cdot \mathbf{v}_{\text{Lag}}$  an estimate of the *speed* of the parameter  $\alpha$ , useful to predict the parameter evolution for the next iteration.

2) *General properties:* The estimation error of the tracking algorithm is defined as:

$$\boldsymbol{\epsilon}(n) = \boldsymbol{\alpha}(n) - \hat{\boldsymbol{\alpha}}_{(n|n)} \quad (11)$$

Combining equations (8) and (10), we have that :

$$\hat{\boldsymbol{\alpha}}_{(n|n)} = \hat{\boldsymbol{\alpha}}_{(n-1|n-1)} + \mu_1 \cdot \mathbf{v}_{\boldsymbol{\epsilon}(n)} + \mu_2 \cdot \mathbf{v}_{\text{Lag}(n-1)} \quad (12)$$

The previous equation confirms that in case of linear drift of the complex amplitudes (*i.e.*  $\boldsymbol{\alpha}(n) = \boldsymbol{\alpha}(n-1) + \text{slope}$ ), it is possible to have no steady state error at the convergence (*i.e.*  $\mathbf{v}_{\boldsymbol{\epsilon}} = \mathbf{0}$  and  $\mathbf{v}_{\text{Lag}} = \frac{1}{\mu_2} \cdot \text{slope}$ ). By using (9), the Z-domain transform of (12) leads to :

$$\hat{\boldsymbol{\alpha}}(z) \cdot [1 - z^{-1}] = [\mu_1 + \frac{\mu_2 \cdot z^{-1}}{1 - z^{-1}}] \cdot \mathbf{v}_{\boldsymbol{\epsilon}}(z) \quad (13)$$

In the following, we note  $F(z) = \mu_1 + \frac{\mu_2 \cdot z^{-1}}{1 - z^{-1}}$  the first-order Lead / Lag filter applied to the error signal in order to obtain  $\hat{\boldsymbol{\alpha}}_{(n|n)}$  by increment from  $\hat{\boldsymbol{\alpha}}_{(n-1|n-1)}$ , according to equation (12). The error signal for each path  $l = 1, \dots, L$  should be in average, proportional to the complex amplitude error for this path in the ideal case<sup>1</sup>. Then we have :

$$v_{\boldsymbol{\epsilon}(n)}^{(l)} = \beta_d^{(l)} \cdot \{\alpha(n) - \hat{\alpha}_{(n|n)}^{(l)}\} + N(n)^{(l)} \quad (14)$$

where  $N(n)^{(l)}$  is a zero-mean disturbance called loop noise. The real coefficient  $\beta_d^{(l)}$  is called the gain of the equivalent complex gain error detector (CGED). In the case where the CGED is the same for each path, (*i.e.*  $\beta_d^{(l)} = \beta_d$ ), the equation (14) leads to the vector formulation :

$$\mathbf{v}_{\boldsymbol{\epsilon}(n)} = \beta_d \cdot \{\boldsymbol{\alpha}(n) - \hat{\boldsymbol{\alpha}}_{(n|n)}\} + \mathbf{N}(n) \quad (15)$$

So, in the Z-transform domain, assuming linear characteristic of the CGED (15), equation (13) leads to

$$\hat{\boldsymbol{\alpha}}(z) = L(z) \cdot \boldsymbol{\alpha}(z) + \frac{L(z)}{\beta_d} \cdot \mathbf{N}(z) \quad (16)$$

where  $L(z)$  is the closed-loop transfer function defined by:

$$L(z) = \frac{\beta_d \cdot F(z)}{1 - z^{-1} + \beta_d F(z)} \quad (17)$$

<sup>1</sup>else we can define an equivalent to the S-curve used in PLL design [12], and (14) will stand only for small errors (linear region of the S-curve).

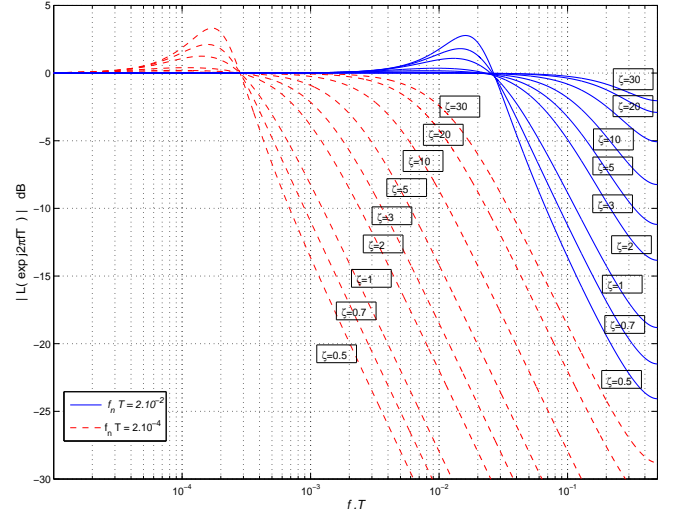


Fig. 1. (exact) Closed loop transfer function  $L(z = e^{j2\pi f T})$  for normalized natural frequency  $f_n T = 2.10^{-2}$  (continuous line) and  $f_n T = 2.10^{-4}$  (dashed line), for various damping factor  $\zeta$ .

Replacing  $F(z)$  by the lead/lag filter expression, we get:

$$L(z) = \frac{\beta_d(\mu_1 - \mu_2) \cdot (1 - z^{-1}) + \beta_d \mu_2}{(1 - z^{-1})^2 + \beta_d(\mu_1 - \mu_2) \cdot (1 - z^{-1}) + \beta_d \mu_2} \quad (18)$$

The condition of stability of the causal rational system  $L(z)$  is obtained when all the roots of the denominator polynomial are inside the unit circle. For a second-order denominator polynomial  $p(z) = (\beta_d \mu_1 + 1) \cdot [1 + c_1 z^{-1} + c_2 z^{-2}]$ , the stability conditions (obtained by the Schur-Cohn test [13]) are :

$$|c_2| < 1 \quad \text{and} \quad -1 < \frac{c_1}{1 + c_2} < 1 \quad (19)$$

with in our case :

$$c_1 = \frac{-2 - \beta_d(\mu_1 - \mu_2)}{\beta_d \mu_1 + 1} \quad \text{and} \quad c_2 = \frac{1}{\beta_d \mu_1 + 1}$$

We can rewrite  $L(z)$  in the frequency-domain, by making  $z = e^{pT}$ , with  $p = j2\pi f$ , and  $f$  is the frequency variable. Assuming slow reaction of the loop during one OFDM symbol  $T$ , the digital loop transfer function is close (approximation  $z^{-1} \approx 1 - pT$ ) to an analog second-order low-pass transfer function parametrized by natural pulsation  $\omega_n$  (or  $f_n = \frac{\omega_n}{2\pi}$ ) and damping factor  $\zeta$ , while  $\omega_n \cdot T \ll 1$  :

$$L(e^{pT}) \approx \frac{2\zeta\omega_n p + \omega_n^2}{p^2 + 2\zeta\omega_n p + \omega_n^2} \quad (20)$$

$$\text{with :} \quad (\omega_n T)^2 = \mu_2 \beta_d \quad (21)$$

$$2\zeta\omega_n T = (\mu_1 - \mu_2)\beta_d \quad (22)$$

The error variance can be numerically computed as  $\sigma_{\boldsymbol{\epsilon}}^2 = \sigma_{\boldsymbol{\epsilon}\alpha}^2 + \sigma_{\boldsymbol{\epsilon}N}^2$ . According to (16) and (11),  $\sigma_{\boldsymbol{\epsilon}\alpha}^2 = \int_{-\frac{1}{2T}}^{+\frac{1}{2T}} \Gamma_{\alpha}(f) \cdot |1 - L(e^{j2\pi f T})|^2 df$  is due to the high-pass filtering<sup>2</sup> of  $\boldsymbol{\alpha}(n)$ , and  $\sigma_{\boldsymbol{\epsilon}N}^2 = \int_{-\frac{1}{2T}}^{+\frac{1}{2T}} \Gamma_N(f) \cdot \frac{1}{\beta_d^2} \cdot |L(e^{j2\pi f T})|^2 df$  is due to the low-pass filtering of  $\mathbf{N}(n)$ . Fig. 1 gives the

<sup>2</sup> $\Gamma_{\alpha}(f)$ ,  $\Gamma_N(f)$  : power spectrum density of  $\sum_l \alpha^{(l)}$  and  $\sum_l N^{(l)}$ .

modulus in frequency-domain of the exact closed-loop filter  $L$  given in (18). The couple  $(f_n, \zeta)$  has to be properly chosen for a good trade-off between gain tracking ability and loop noise reduction, for a given SNR and  $f_d T$  scenario.

**Special case of first-order loop:** if  $\mu_2 = 0$ , equations are reduced to  $L(z) = \frac{\beta_d \mu_1}{(1-z^{-1}) + \beta_d \mu_1}$  and then approximatively to a first-order low-pass transfer function :  $L(e^{pT}) \approx \frac{\omega_c}{p + \omega_c}$  with cut-off frequency  $\omega_c$  such that

$$(\omega_c T) = \mu_1 \beta_d \quad (23)$$

### B. First algorithm :

1) *Motivation:* for each OFDM symbol, the Squares Error (SE) for the received pilot subcarriers is defined by :

$$S(\hat{\alpha}_{(n)}) = \zeta_{(n)}^H \cdot \zeta_{(n)} \quad (24)$$

where the  $N_p \times 1$  error vector is

$$\zeta_{(n)} = \mathbf{y}_{\mathbf{p}(n)} - \text{diag}\{\mathbf{x}_{\mathbf{p}(n)}\} \mathbf{F}_{\mathbf{p}} \hat{\alpha}_{(n)} \quad (25)$$

The LS-estimator of  $\alpha_{(n)}$  is :

$$\mathbf{a}_{\text{LS}(n)} = \mathbf{G}_{(n)} \mathbf{y}_{\mathbf{p}(n)} \quad (26)$$

where

$$\mathbf{G}_{(n)} = (\mathbf{F}_{\mathbf{p}}^H \text{diag}\{\mathbf{x}_{\mathbf{p}(n)}\}^H \text{diag}\{\mathbf{x}_{\mathbf{p}(n)}\} \mathbf{F}_{\mathbf{p}})^{-1} \mathbf{F}_{\mathbf{p}}^H \text{diag}\{\mathbf{x}_{\mathbf{p}(n)}\}^H \quad (27)$$

And assuming normalized QPSK data, the matrix inversion should be done only once (independent of the index  $n$ ):

$$\mathbf{G}_{(n)} = (\mathbf{F}_{\mathbf{p}}^H \mathbf{F}_{\mathbf{p}})^{-1} \mathbf{F}_{\mathbf{p}}^H \text{diag}\{\mathbf{x}_{\mathbf{p}(n)}\}^H \quad (28)$$

Thus, after LS estimation, we obtain :

$$\mathbf{a}_{\text{LS}(n)} = \alpha_{(n)} + \epsilon_{\mathbf{w}(n)} \quad (29)$$

where  $\epsilon_{\mathbf{w}(n)}$  is a zero-mean complex Gaussian noise vector with correlation matrix  $E\{\epsilon_{\mathbf{w}(n)} \cdot \epsilon_{\mathbf{w}(n)}^H\} = \sigma^2 \cdot (\mathbf{F}_{\mathbf{p}}^H \mathbf{F}_{\mathbf{p}})^{-1}$

2) *Error signal for the first Algorithm:* We use the difference between the LS estimator  $\mathbf{a}_{\text{LS}(n)}$  for the  $n$ th OFDM block and the predicted vector for this block,  $\hat{\alpha}_{(n|n-1)}$ . The error signal vector is then :

$$\mathbf{v}_{\epsilon(n)} = \mathbf{G}_{(n)} \mathbf{y}_{\mathbf{p}(n)} - \hat{\alpha}_{(n|n-1)} \quad (30)$$

3) *Analysis and loop coefficients tuning:* Now, for the specific case of the first error signal defined in (30), we have from equations (26),(29),(8) that:

$$\mathbf{v}_{\epsilon}(z) = (\alpha(z) + \epsilon_{\mathbf{w}}(z)) - (\hat{\alpha}(z) - \mu_1 \cdot \mathbf{v}_{\epsilon}(z)) \quad (31)$$

leading to

$$\mathbf{v}_{\epsilon}(z) = \frac{\alpha(z) - \hat{\alpha}(z)}{1 - \mu_1} + \frac{\epsilon_{\mathbf{w}}(z)}{1 - \mu_1} \quad (32)$$

We can conclude than the linear model (15) is strictly valid for the first algorithm, with a CGED gain given by :

$$\beta_d = \frac{1}{1 - \mu_1} \quad (33)$$

and a loop noise equal to  $N_{(n)} = \beta_d \cdot \epsilon_{\mathbf{w}(n)}$ . For the first algorithm, the stability conditions (19) are then:

$$0 < \mu_1 < 2 \quad \text{and} \quad 0 \leq \mu_2 < 4 - 2\mu_1$$

And from (21) and (22), one given couple  $(\omega_n, \zeta)$  of the second-order low-pass transfer function can be obtained in tuning  $(\mu_1, \mu_2)$  as :

$$\mu_1 = \frac{(\omega_n T)^2 + 2\zeta \omega_n T}{1 + (\omega_n T)^2 + 2\zeta \omega_n T} \quad (34)$$

$$\mu_2 = \frac{(\omega_n T)^2}{1 + (\omega_n T)^2 + 2\zeta \omega_n T} \quad (35)$$

In this way, we finally have :  $0 \leq \mu_2 < \mu_1 \leq 1$ .

**Special case of first-order loop :** if gain  $\mu_2 = 0$ , the on-line estimation algorithm is reduced to an order 1 AR low-pass filtering of the LS estimator  $\mathbf{a}_{\text{LS}(n)}$ :

$$\hat{\alpha}_{(n|n)} = (1 - \mu_1) \cdot \hat{\alpha}_{(n-1|n-1)} + \mu_1 \cdot \mathbf{a}_{\text{LS}(n)} \quad (36)$$

We have from (23) that  $\mu_1 = \frac{\omega_c T}{1 + \omega_c T}$ .

### C. Second algorithm

1) *Motivation:* Instead of computing explicitly the LS estimator  $\mathbf{a}_{\text{LS}(n)}$  for each OFDM block, we can look for an iterative steepest descent procedure. In this way, we use same error signal that for an LMS (Least Mean Squares) algorithm, but inserted in a second-order loop versus a first-order loop. This means finally to use the prediction in order to improve LMS-type adaptive algorithm as in [10]. Applying the stochastic gradient descent method means to take the partial derivatives of the SE,  $S(\hat{\alpha})$ , defined in (24) with respect to the individual entries of the vector  $\hat{\alpha}$ :

$$\nabla_{\hat{\alpha}}(S(\hat{\alpha})) = 2 \cdot \nabla_{\hat{\alpha}}(\zeta^H) \cdot \zeta \quad (37)$$

where the  $L \times N_p$  matrix  $\nabla_{\hat{\alpha}}(\zeta^H)$  contains in one given column the partial derivatives (relative to the components of  $\hat{\alpha}$ ) for the corresponding pilot subcarrier. We obtain

$$\nabla_{\hat{\alpha}}(S(\hat{\alpha})) = -2 \cdot \mathbf{F}_{\mathbf{p}}^H \text{diag}\{\mathbf{x}_{\mathbf{p}}\}^H \cdot \{\mathbf{y}_{\mathbf{p}} - \text{diag}\{\mathbf{x}_{\mathbf{p}}\} \mathbf{F}_{\mathbf{p}} \hat{\alpha}\} \quad (38)$$

The successive corrections to the weight vector  $\hat{\alpha}$  must then be in direction opposite to the gradient vector  $\nabla_{\hat{\alpha}}(S(\hat{\alpha}))$ .

2) *Error signal for the second Algorithm:* Inserted in the global structure of the tracking procedure, the error signal for the  $n$ th OFDM symbol is chosen proportional to the negative of the gradient vector of the SE predicted for this block, from the  $(n-1)$ th observation block:

$$\mathbf{v}_{\epsilon(n)} = \mathcal{K}_{(n)}^H \cdot \{\mathbf{y}_{\mathbf{p}(n)} - \mathcal{K}_{(n)} \hat{\alpha}_{(n|n-1)}\} \quad (39)$$

where we define the  $N_p \times L$  matrix  $\mathcal{K}_{(n)} = \text{diag}\{\mathbf{x}_{\mathbf{p}(n)}\} \mathbf{F}_{\mathbf{p}}$ . So, if  $\mu_2 = 0$ , the second tracking algorithm is exactly an LMS algorithm, with  $\mu_1$  as step-size parameter (and with  $\hat{\alpha}_{(n|n-1)} = \hat{\alpha}_{(n-1|n-1)}$ ).

3) *Analysis and loop coefficients tuning*: Using the observation equation (5), the error signal (39) can be rewritten:

$$\mathbf{v}_{\epsilon(n)} = \mathcal{K}_{(n)}^H \mathcal{K}_{(n)} \{\boldsymbol{\alpha}_{(n)} - \hat{\boldsymbol{\alpha}}_{(n|n-1)}\} + \mathcal{K}_{(n)}^H \cdot \mathbf{w}_{\mathbf{p}(n)} \quad (40)$$

Using (8), the error signal versus the error  $\epsilon_{(n)}$  becomes :

$$\mathbf{v}_{\epsilon(n)} = [I - \mu_1 \cdot \boldsymbol{\Gamma}]^{-1} \boldsymbol{\Gamma} \cdot \{\boldsymbol{\alpha}_{(n)} - \hat{\boldsymbol{\alpha}}_{(n|n-1)}\} + [I - \mu_1 \cdot \boldsymbol{\Gamma}]^{-1} \mathcal{K}_{(n)}^H \cdot \mathbf{w}_{\mathbf{p}(n)} \quad (41)$$

where the  $L \times L$  Hermitian matrix  $\boldsymbol{\Gamma} = \mathcal{K}_{(n)}^H \mathcal{K}_{(n)}$  is independent of index  $n$  when assuming normalized data symbols, with elements defined by  $[\boldsymbol{\Gamma}]_{ll'} = \sum_{k=1}^{N_p} e^{j2\pi(\tau_l - \tau_{l'})}$ . This elements are identical on the diagonal, equal to  $[\boldsymbol{\Gamma}]_{ll} = N_p$ . Eq. (41) indicates that the CGED output of one given desired path may be influenced by an interference term depending on adjacent paths. This “inter-path interference” may increase the variance of the loop noise if the Hermitian matrix  $\boldsymbol{\Gamma}$  is not a diagonally dominant matrix. This condition depends only on the delays distribution. If non-diagonal terms can be neglected, and if  $\mu_1 N_p \ll 1$ , the detector gain is approximatively:

$$\beta_d \approx \frac{N_p}{1 - \mu_1 N_p} \quad (42)$$

and according to (21)(22), the tuning of the coefficient of the second-order equivalent closed loop is given by replacing  $(\mu_1, \mu_2)$  by  $(N_p \mu_1, N_p \mu_2)$  in equations (34)(35). In this way, we finally have :  $0 \leq \mu_2 < \mu_1 \leq 1/N_p$ .

#### IV. REFERENCE ALGORITHM : KALMAN FILTER

In order to compare the performance of the previous simple sub-optimal algorithms, we recall here the Kalman Filter processing, which can give the optimal performance for a so-called Linear Gaussian Problem [11]. The Kalman filter is a recursive algorithm composed of two stages: Time Update Equations and Measurement Update Equations. In order to use Kalman filter, we first have to give a linear state-space representation of the problem. Classically, the flat fading Rayleigh channel can be well approached [8] by an Auto-regressive (AR) model. Most often, a first-order AR (AR1) model is used to model the variation of each path,  $\alpha_l^{(n)}$  as :

$$\alpha_l^{(n)} = \gamma \cdot \alpha_l^{(n-1)} + u_l^{(n)}$$

where  $\gamma = J_0(2\pi f_d T)$  according to the Jakes’ model, and  $u_l^{(n)}$  is zero mean Gaussian complex circular with a variance  $\sigma_{u_l}^2 = \sigma_{\alpha_l}^2 (1 - \gamma^2)$ . Based on the previous AR1 model of the gains evolution, the two stages of the so called *AR1-Kalman* algorithm are defined as:

##### Time Update Equations:

$$\begin{aligned} \hat{\boldsymbol{\alpha}}_{(n|n-1)} &= \gamma \cdot \hat{\boldsymbol{\alpha}}_{(n-1|n-1)} \\ \mathbf{P}_{(n|n-1)} &= \gamma^2 \cdot \mathbf{P}_{(n-1|n-1)} + \mathbf{U} \end{aligned} \quad (43)$$

##### Measurement Update Equations:

$$\begin{aligned} \mathbf{K}_{(n)} &= \mathbf{P}_{(n|n-1)} \mathcal{K}_{(n)}^H (\mathcal{K}_{(n)} \mathbf{P}_{(n|n-1)} \mathcal{K}_{(n)}^H + \sigma^2 \mathbf{I}_{N_p})^{-1} \\ \hat{\boldsymbol{\alpha}}_{(n|n)} &= \hat{\boldsymbol{\alpha}}_{(n|n-1)} + \mathbf{K}_{(n)} (\mathbf{y}_{\mathbf{p}(n)} - \mathcal{K}_{(n)} \hat{\boldsymbol{\alpha}}_{(n|n-1)}) \\ \mathbf{P}_{(n|n)} &= \mathbf{P}_{(n|n-1)} - \mathbf{K}_{(n)} \mathcal{K}_{(n)} \mathbf{P}_{(n|n-1)} \end{aligned} \quad (44)$$

where  $\mathbf{K}_{(n)}$  is the Kalman gain matrix and  $\mathbf{U} = \text{diag}\{\sigma_{u_1}^2, \dots, \sigma_{u_L}^2\}$ . Note that the equations are similar to those of the second (LMS-based) algorithm with  $\mu_2 = 0$  by replacing the Kalman gain  $\mathbf{K}_{(n)}$  by  $\mu_1 \cdot \mathcal{K}_{(n)}^H$ , which requires an additional matrix inversion at each iteration.

#### V. SIMULATIONS

In this section, the performance of the recursive algorithms is evaluated and compared to that of reference algorithms (LS and Kalman algorithms). The normalized channel model is GSM Rayleigh model [9] [6] with  $L = 6$  paths and maximum delay  $\tau_{max} = 10T_s$ . A 4QAM-OFDM system with normalized symbols,  $N = 128$  subcarriers,  $N_g = \frac{N}{8}$  subcarriers,  $N_p = 16$  pilots (*i.e.*,  $L_f = 8$ ) and  $\frac{1}{T_s} = 2MHz$  is used. The MSE and the BER are evaluated under a slowly time-varying channel with  $f_d T = 10^{-2}$  (corresponding to a vehicle speed  $V_m \approx 140 km/h$  for  $f_c = 1GHz$ ). Table I gives the loop coefficients used, that yield around the best possible performance for the proposed algorithms.

SNR	0dB	5dB	10dB	15dB	25dB	35dB
$f_n$ (Algo 1)	$2f_d$	$2.5f_d$	$3f_d$	$4f_d$	$6f_d$	$15f_d$
$\zeta$	0.5	0.5	0.5	0.5	0.5	0.3
$f_n$ (Algo 2)	$7f_d$	$8f_d$	$10f_d$	$15f_d$	$20f_d$	$23f_d$

TABLE I  
LOOP COEFFICIENTS (FIRST / SECOND ALGORITHM)

Fig. 2 shows the evolution of MSE versus SNR. First of all, we observe that the performance of the AR1-Kalman algorithm, despite its complexity, does not reach the BRCB [2] in the case of a slowly channel variation with  $f_d T = 10^{-2}$ . This may be due to the difference between the real (Jakes) channel model and approached (AR1) model used in the Kalman filter (actually AR1-Kalman algorithm would reach the associated BCRB if the channel was exactly an AR1 based channel).

Secondly, for the first (LS-based) proposed algorithm, it is observed that with a first-order loop (with  $\mu_1 = 1$  and  $\mu_2 = 0$ ) the MSE is very close to the error obtained by the AR1-Kalman filter, especially for large SNRs. On the other hand, it is interesting to observe that for a second-order loop with the best loop parameters (Table I), the MSE is closer to the BCRB than for AR1-Kalman algorithm. According to Fig. 1, the closed loop transfer function for low SNRs, with the set of values ( $\zeta = 0.5; f_n T = 2f_d T$ ), approaches the Jakes Doppler spectrum shape. And for high SNRs, the set of values ( $\zeta = 0.3; f_n T = 15f_d T$ ) permits to obtain a very large loop bandwidth. The corresponding loop coefficients are ( $\mu_1 = 0.124; \mu_2 = 0.0138$ ) for SNR = 0dB, and ( $\mu_1 = 0.647; \mu_2 = 0.314$ ) for SNR = 35 dB. It is then observed that the best performance are always obtained with a damping factor around  $\zeta = 0.5$  (and even less in high SNRs Region). This point reveals the advantage of a second-order loop versus a first-order loop (*i.e.*  $\mu_2 = 0$ ). It emphasizes then the benefit of the integration, that is inherent to the second-order loop, but not included in the AR1-Kalman algorithm. Of course, in the Kalman algorithm, larger AR model orders could be used

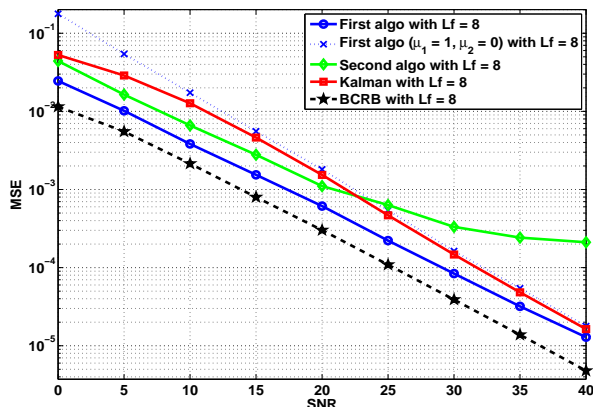


Fig. 2. MSE vs SNR for  $f_d T = 10^{-2}$

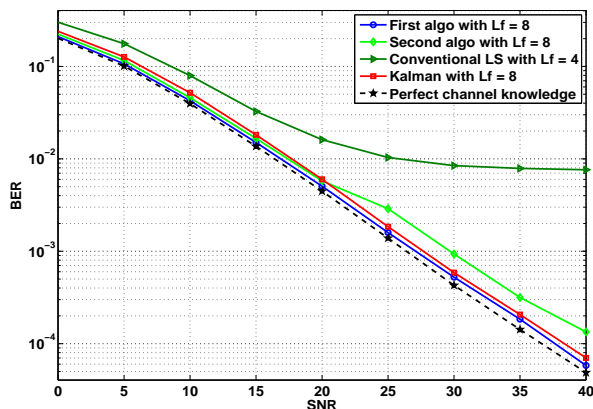


Fig. 3. BER vs SNR for  $f_d T = 10^{-2}$

to reduce the mismatch with the true channel (in predicting also the slope) and go toward optimal performance, but at the expense of the complexity.

Finally, for the second (LMS-based) algorithm, the MSE is larger than that of the first algorithm but is lower than that of the AR1-Kalman for low and moderate SNRs. According to the theoretical analysis, this is due to a non favorable distribution of the delays for the Rayleigh channel. The non diagonal dominant property of the matrix  $\Gamma$  for the Rayleigh channel (ratio between the energy of the main and secondary diagonal is only around 1.3) yields “interpath interference” (IPI) which increases the loop noise variance. For high SNRs, the error variance reaches a floor, since the IPI becomes dominant with respect to the additive noise. The best choice of the natural frequency  $f_n$ , according to table I, seems different than that of the first algorithm, but the computation is also much less reliable because of the bad linear approximation (42) in presence of IPI.

Fig. 3 gives the BER performance of our algorithms for  $f_d T = 10^{-2}$  (using a Zero-Forcing Equalizer), compared to the conventional algorithms of [1] (LS criterion based only on the current symbol, with low-pass frequency interpolation (LPI)). For the sake of comparison, we also plotted the BER obtained with perfect knowledge of the channel. It is obvious that our algorithms outperform the conventional method, since

we use the previous symbols in estimation process. Moreover, the BER results of our algorithms, the AR1-kalman and the reference (perfect knowledge of channel) agree with the MSE results. The BER performance of the different algorithms is very close due to the use of QPSK symbols.

## VI. CONCLUSION

Sub-optimal path complex gains estimation techniques for OFDM systems over slow-fading channels have been proposed. The methods are designed for the comb pilot pattern (*i.e.* each OFDM symbol carries equi-spaced pilot subcarriers) but can easily be generalized to others frequencies-time grid pilot patterns. Our algorithms require path delay information, that can be accurately obtained as in [4] [7]. The key is to capitalize on the invariance of the delays of the channel during a large number of OFDM symbols. When combined with past estimations through a simple second-order recursive loop, this allows to improve the tracking of complex amplitudes from the delays related information. The performance has been evaluated through simulations in terms of the MSE and BER, demonstrating the considerable benefits of the proposed algorithm compared to conventional methods. Moreover, without using accurate *a priori* information about channel statistics, the performance is comparable (and even better for the first algorithm) to the more complex Kalman estimator, when the later is based only on a first-order Auto-regressive approximation of the true channel.

## REFERENCES

- [1] M. Hsieh and C. Wei, “Channel estimation for OFDM systems based on comb-type pilot arrangement in frequency selective fading channels” in *IEEE Trans. Consumer Electron.*, vol.44, no. 1, Feb. 1998.
- [2] H. Hijazi and L. Ros, “Analytical analysis of Bayesian Cramer-Rao Bound for dynamical Rayleigh channel complex gains estimation in OFDM systems” in *IEEE Trans. Signal Process.*, Vol. 57, no. 5, May 2009.
- [3] W. Chen and R. Zhang, “Kalman filter Channel estimator for OFDM systems in time and frequency-selective fading environment” in *ICASSP*, Vol. 4, pp. 17-21, May 2004.
- [4] B. Yang, K. B. Letaief, R. S. Cheng and Z. Cao, “Channel estimation for OFDM transmission in multipath fading channels based on parametric channel modeling” in *IEEE Trans. Commun.*, vol. 49, no. 3, pp. 467-479, March 2001.
- [5] O. Simeone, Y. Bar-Ness and U. Spagnolini “Pilot-Based Channel Estimation for OFDM Systems by Tracking the Delay-Subspace” in *IEEE Trans. on Wireless Commun.*, vol. 3, no. 3, pp. 315-325, January 2004.
- [6] H. Hijazi and L. Ros, “Polynomial estimation of time-varying multi-path gains with intercarrier interference mitigation in OFDM systems” in *IEEE Trans. Vehicular Techno.*, Vol. 58, no. 1, pp.140-151, Jan. 2009.
- [7] H. Hijazi, L. Ros, “Joint Data QR-Detection and Kalman Estimation for OFDM Time-varying Rayleigh Channel Complex Gains” in *IEEE Trans. On Communications*, accepted, to be appeared in 2010.
- [8] H. Wang and P.Chang, “On verifying the first-order Markovian assumption for a Rayleigh fading channel model” in *IEEE Trans. Vehicular Technology*, vol. 45, pp. 353-357, May 1996.
- [9] Y. Zhao and A. Huang, “A novel Channel estimation method for OFDM Mobile Communications Systems based on pilot signals and transform domain processing” in *Proc. IEEE 47th Vehicular Techno. Conf.*, Phoenix, USA, May 1997, pp. 2089-2093.
- [10] S. Gazor, “Prediction in LMS-type Additive Algorithms for Smoothly Time Varying Environments” in *IEEE Trans. Signal Processing*, vol. 47, n. 6, pp. 1735-1739, June 1999.
- [11] S. Haykin, *Adaptive Filter Theory*. Prentice Hall, 2002,
- [12] U. Mengali, A.N. D’Andrea, *Synchronization Techniques for Digital Receivers (Applications of Communications Theory)*. PLENUM, 1997.
- [13] B. Porat, *A course in digital signal processing*. Wiley, 1997.